

# $n$ -CPS: Generalising Cross Pseudo Supervision to $n$ Networks for Semi-Supervised Semantic Segmentation

Dominik Filipiak<sup>1,2</sup>, Piotr Tempczyk<sup>1,3</sup>, Marek Cygan<sup>3</sup>

<sup>1</sup> AI Clearing, Inc.

<sup>2</sup> Semantic Technology Institute, Department of Computer Science, University of Innsbruck

<sup>3</sup> Institute of Informatics, University of Warsaw

{df, pt}@aiclearing.com, cygan@mimuw.edu.pl

## Abstract

We present  $n$ -CPS – a generalisation of the recent state-of-the-art cross pseudo supervision (CPS) approach for the task of semi-supervised semantic segmentation. In  $n$ -CPS, there are  $n$  simultaneously trained subnetworks that learn from each other through one-hot encoding perturbation and consistency regularisation. We also show that ensembling techniques applied to subnetworks outputs can significantly improve the performance. To the best of our knowledge,  $n$ -CPS paired with CutMix outperforms CPS and sets the new state-of-the-art for Pascal VOC 2012 with (1/16, 1/8, 1/4, and 1/2 supervised regimes) and Cityscapes (1/16 supervised). The code is available on GitHub<sup>1</sup>.

## 1 Introduction

An intense research effort can be observed in data- and label-efficient machine learning. The latter can be tackled using the semi-supervised learning task. Semantic segmentation can significantly benefit from semi-supervised methods due to the relatively high cost of labelling every pixel. Among numerous techniques, consistency regularisation is proven to improve performance in such settings. The recent cross pseudo supervision (abbreviated as CPS) approach [Chen *et al.*, 2021] has set the new state-of-the-art in the task of semi-supervised semantic segmentation. It simultaneously trains two networks, which are penalised for discrepancies between them. This consistency regularisation mechanism is enriched with a specific one-hot encoding data perturbation. This paper proposes a generalised cross pseudo supervision approach, which can handle more than two networks in the data augmentation process. Our contribution is two-fold:

- we generalise the CPS to handle more than two networks in the training process,
- we propose an ensemble learning inspired approach to evaluation, which treats these networks as a blend of weak learners and acts as a strong one.

<sup>1</sup>The code will be released after the publication. For reviewers, it is available as supplementary material.

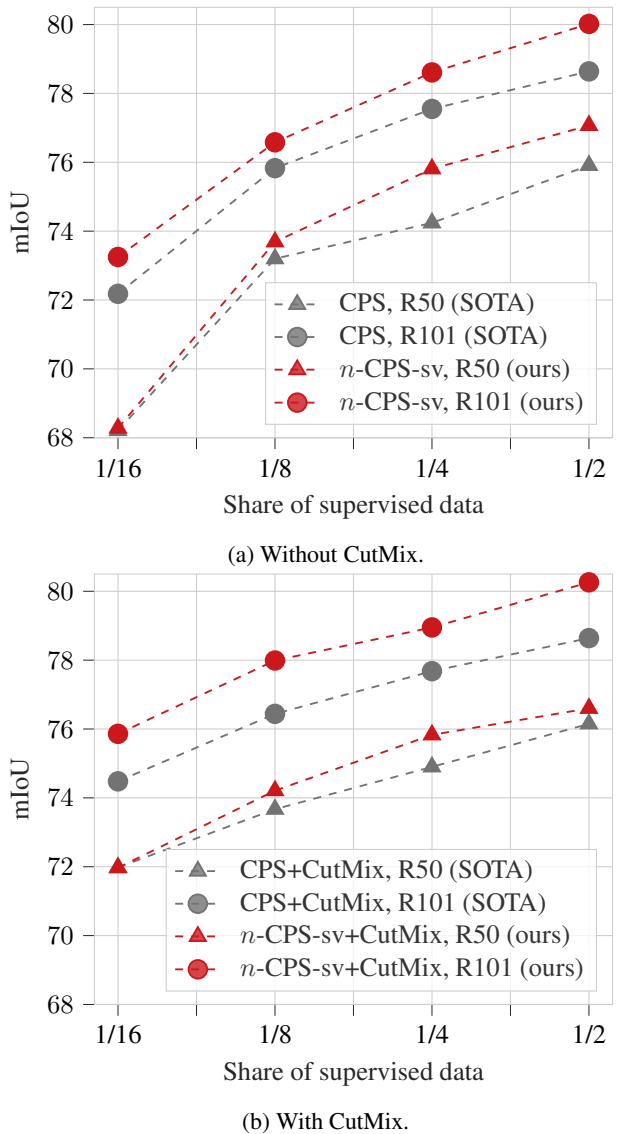


Figure 1: Our method ( $n$ -CPS-sv,  $n = 3$ ) on the Pascal VOC 2012 dataset, compared to the state-of-the-art CPS [Chen *et al.*, 2021]. R50 and R101 denote ResNet-50 and ResNet-101 respectively.

To the best of our knowledge,  $n$ -CPS paired with CutMix [Yun *et al.*, 2019] outperforms CPS and sets the new state-of-the-art for Pascal VOC 2012 for 1/16, 1/8, 1/4, and 1/2 supervised regimes and Cityscapes for 1/16 supervised data. Figure 1 presents results for the Pascal VOC 2012 dataset.

The paper is structured as follows. In the Section 2, we present  $n$ -CPS, the proposed method. The results of evaluation are presented Section 3 – the experiment setup in Section 3.1, comparison with the state-of-the art in Section 3.2, and ablation studies in Section 3.3. Section 4 offers a comprehensive literature review of the literature on the topic. The paper is concluded with a short summary in Section 5.

## 2 Method

This section describes the proposed method. Firstly, we present plain  $n$ -CPS. Then, we introduce a variant paired with the CutMix algorithm. Finally, we present ensemble learning techniques, which increases the evaluation performance.

**$n$ -CPS.** The proposed method generalises the cross pseudo supervision (CPS) approach for semi-supervised semantic segmentation. Similarly to CPS, a key feature of  $n$ -CPS is consistency regularisation between the output of one network and the output of another one perturbed with pixel-wise one-hot encoding. This perturbation (denoted as  $\max$  hereafter) sets 1 for the class with the highest probability and 0 for the others. However, instead of using two networks (with the same architecture but initialised differently),  $n$  can be used in  $n$ -CPS (setting  $n$  to 2 results in the original CPS approach). Let  $\mathcal{D}_L$  and  $\mathcal{D}_U$  denote labelled and unlabelled training data sets respectively, both containing images of size  $W \times H$ . The  $n$ -CPS architecture consists of a set of  $n$  networks  $f$ , each with the same architecture but initialised with different set of parameters from  $\Theta = \{\theta_1, \theta_2, \dots, \theta_n\}$ . The output of the  $j$ -th network  $f(\mathbf{x}; \theta_j)$  on the  $i$ -th pixel of the image  $\mathbf{x}$  is represented by  $\mathbf{p}_{ij}$ . The supervised loss is calculated in a standard way:

$$\mathcal{L}_L = \frac{1}{|\mathcal{D}_L|} \sum_{\mathbf{x} \in \mathcal{D}_L} \frac{1}{W \times H} \sum_{i=1}^{W \times H} \sum_{j=1}^n l(\mathbf{p}_{ij}, \mathbf{y}_i^*), \quad (1)$$

where  $l$  is the loss function (we used the standard cross-entropy loss). The ground truth for the labelled data is marked as  $\mathbf{y}_i^*$ . For the CPS loss for labelled and unlabelled data, we use the following definitions respectively:

$$\mathcal{L}_{CPS}^L = \frac{1}{|\mathcal{D}_L|} \sum_{\mathbf{x} \in \mathcal{D}_L} \frac{1}{W \times H} \sum_{i=1}^{W \times H} \sum_{j=1}^n \frac{1}{n-1} \sum_{k \neq j}^n l(\mathbf{p}_{ij}, \mathbf{y}_{ik}), \quad (2)$$

$$\mathcal{L}_{CPS}^U = \frac{1}{|\mathcal{D}_U|} \sum_{\mathbf{x} \in \mathcal{D}_U} \frac{1}{W \times H} \sum_{i=1}^{W \times H} \sum_{j=1}^n \frac{1}{n-1} \sum_{k \neq j}^n l(\mathbf{p}_{ij}, \mathbf{y}_{ik}). \quad (3)$$

This time the loss is calculated with  $\mathbf{y}_{ik}$ , which is the one-hot encoded output of the  $k$ -th network on the unlabelled data. Finally, the overall loss  $\mathcal{L}$  is defined as:

$$\mathcal{L} = \mathcal{L}_L + \lambda (\mathcal{L}_{CPS}^L + \mathcal{L}_{CPS}^U), \quad (4)$$

---

### Algorithm 1 $n$ -CPS

---

```

1: for each batch do
2:    $\mathcal{L} \leftarrow 0$ ,  $\mathcal{L}_L \leftarrow 0$ ,  $\mathcal{L}_{CPS}^L \leftarrow 0$ ,  $\mathcal{L}_{CPS}^U \leftarrow 0$ 
3:    $\mathbf{x}^L, \mathbf{x}^U, \mathbf{Y}^* \leftarrow \text{dataloader.} \text{iter}()$ 
4:   for  $i = 1, \dots, n$  do
5:      $\mathbf{P}_i^L \leftarrow f(\mathbf{x}^L; \theta_i)$ 
6:      $\mathbf{P}_i^U \leftarrow f(\mathbf{x}^U; \theta_i)$ 
7:   end for
8:   for  $(l, r) \in \binom{n}{2}$  do
9:      $\mathbf{Y}_l^U \leftarrow \max(\mathbf{P}_l^U)$ ,  $\mathbf{Y}_r^U \leftarrow \max(\mathbf{P}_r^U)$  //  $\mathcal{X}$ 
10:     $\mathbf{Y}_l^L \leftarrow \max(\mathbf{P}_l^L)$ ,  $\mathbf{Y}_r^L \leftarrow \max(\mathbf{P}_r^L)$  //  $\mathcal{X}$ 
11:     $\mathcal{L}_{CPS}^L \leftarrow \mathcal{L}_{CPS}^L + \mathcal{L}_{CPS}(\mathbf{P}_l^U, \mathbf{Y}_r) + \mathcal{L}_{CPS}(\mathbf{P}_r^U, \mathbf{Y}_l)$ 
12:     $\mathcal{L}_{CPS}^U \leftarrow \mathcal{L}_{CPS}^U + \mathcal{L}_{CPS}(\mathbf{P}_l^L, \mathbf{Y}_r) + \mathcal{L}_{CPS}(\mathbf{P}_r^L, \mathbf{Y}_l)$ 
13:   end for
14:   for  $i = 1, \dots, n$  do
15:      $\mathcal{L}_L \leftarrow \mathcal{L}_L + \mathcal{L}_L(\mathbf{P}_i^L, \mathbf{Y}^*)$ 
16:   end for
17:    $\mathcal{L} \leftarrow \mathcal{L}_L + \frac{\lambda}{(n-1)} (\mathcal{L}_{CPS}^U + \mathcal{L}_{CPS}^L)$ 
18:    $\mathcal{L}.\text{backward}()$ 
19: end for

```

---

where  $\lambda$  is the weight of CPS loss. Figure 2 depicts calculating the CPS loss.

Details are presented in Algorithm 1. In each batch, we select images from the labelled and unlabelled data set, which are denoted as  $\mathbf{x}^L, \mathbf{x}^U$  respectively. Then, we perform the forward passes on all the data using all the networks separately. The  $n$ -CPS model consists of  $n$  networks, and the output of each network is the pixel-wise probability of each class. The  $i$ -th one is represented by  $f(\cdot; \theta_i)$ . Then, we perform the cross pseudo supervision for each unique pair of networks  $\binom{n}{2}$  times. The one-hot encoded outputs of the  $l$ -th and  $r$ -th networks are denoted as  $\mathbf{Y}_l$  and  $\mathbf{Y}_r$ . In this case,  $\max$  is a pixel-wise maximum function that selects each pixel's maximum value from the two masked images. It is calculated without passing the gradient (denoted as  $\mathcal{X}$  in the algorithm). The CPS loss is performed both on the labelled and unlabelled data. Then, we calculate the standard supervised loss for each network. The overall loss consists of the standard labelled loss  $\mathcal{L}_L$  and the CPS losses  $\mathcal{L}_{CPS}^L$  and  $\mathcal{L}_{CPS}^U$  (for labelled and unlabelled data weighted by  $\lambda$  and normalised by the factor of  $\frac{1}{n-1}$ ). While  $n$ -CPS needs  $\binom{n}{2}$  CPS loss calculations per batch, the most computationally expensive forward calls are hit only  $2n$  times per batch, which *effectively* makes the time complexity of the algorithm linear in  $n$ .

**$n$ -CPS with CutMix.** We also used the CutMix augmentation algorithm [Yun *et al.*, 2019] adapted to semantic segmentation [French *et al.*, 2019], as it was proven to be very effective in the original CPS approach [Chen *et al.*, 2021]. Algorithm 2 presents our method. In each batch, we select images from the labelled and unlabelled data set, and we randomly select a binary mask  $M$ . Regarding the data,  $\mathbf{x}^L, \mathbf{x}^U, \mathbf{x}^m$  represent the labelled, unlabelled and mixed data respectively. Notice that there are two different sets of unlabelled data,  $\mathbf{x}_1^U$  and  $\mathbf{x}_2^U$ . They both are used to generate the mixed data  $\mathbf{x}^m$ , which is the result of the CutMix applied with

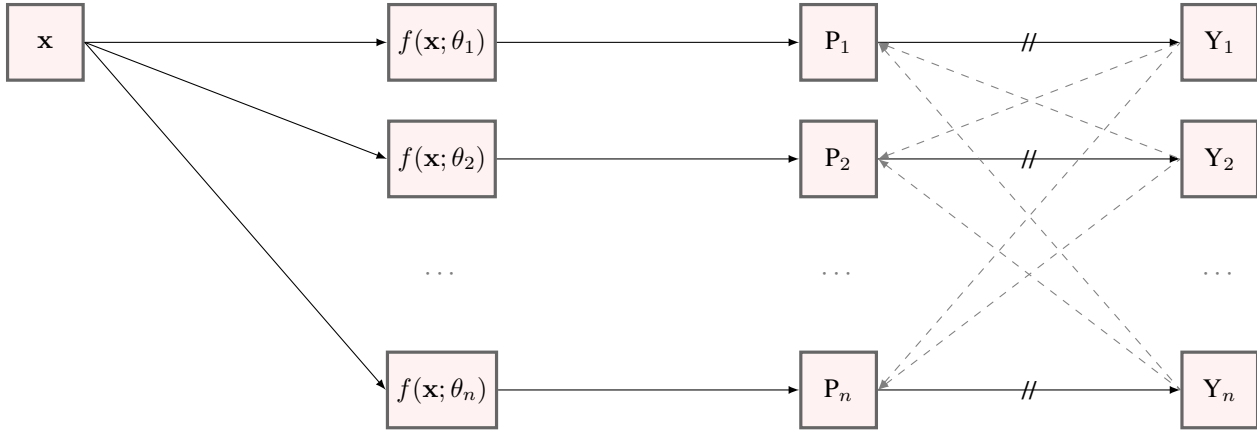


Figure 2: The architecture of  $n$ -CPS during the CPS loss calculation. The slashed line (with  $\text{//}$ ) represents not passing the gradient, whereas the dashed line (---) denotes cross-pseudo supervision.

batch-wise mask  $\mathbf{M}$ . The mask is the same size as the image and is randomly generated to satisfy CutMix constraints.

Then, we perform the forward passes on all the data using all the networks separately, similarly to  $n$ -CPS. Cross pseudo supervision for each unique pair of networks is performed slightly differently regarding one-hot encoding vectors. They are obtained by combining images in a CutMix-like approach and applying the maximum function. The overall loss consists of the standard labelled loss  $\mathcal{L}_L$  and the CPS loss  $\mathcal{L}_{\text{CPS}}^U$  weighted by  $\lambda$  and normalised by the factor of  $\frac{1}{n-1}$ . Similarly to the original CPS with CutMix augmentation, the CPS loss is not calculated on supervised data and therefore  $\mathcal{L}_{\text{CPS}}^L$  is not calculated. Once again, forward calls are linear in  $n$  and setting  $n = 2$  results in the original CPS+CutMix approach.

#### Algorithm 2 $n$ -CPS+CutMix

```

1: for each batch do
2:    $\mathcal{L} \leftarrow 0$ ,  $\mathcal{L}_L \leftarrow 0$ ,  $\mathcal{L}_{\text{CPS}}^U \leftarrow 0$ 
3:    $\mathbf{x}^L, \mathbf{x}_1^U, \mathbf{x}_2^U, \mathbf{M}, \mathbf{Y}^* \leftarrow \text{dataloader}.iter()$ 
4:    $\mathbf{x}^m \leftarrow \text{CutMix}(\mathbf{x}_1^U, \mathbf{x}_2^U, \mathbf{M})$ 
5:   for  $i = 1, \dots, n$  do
6:      $\mathbf{P}_i^L \leftarrow f(\mathbf{x}^L; \theta_i)$ 
7:      $\mathbf{P}_i^m \leftarrow f(\mathbf{x}^m; \theta_i)$ 
8:      $\mathbf{P}_{i,1}^U \leftarrow f(\mathbf{x}_1^U; \theta_i)$ 
9:      $\mathbf{P}_{i,2}^U \leftarrow f(\mathbf{x}_2^U; \theta_i)$ 
10:   end for
11:   for  $(l, r) \in \binom{n}{2}$  do
12:      $\mathbf{Y}_l \leftarrow \max(\mathbf{P}_{l,1}^U \odot (1 - \mathbf{M}) + \mathbf{P}_{l,2}^U \odot \mathbf{M}) \text{//} \mathcal{X}$ 
13:      $\mathbf{Y}_r \leftarrow \max(\mathbf{P}_{r,1}^U \odot (1 - \mathbf{M}) + \mathbf{P}_{r,2}^U \odot \mathbf{M}) \text{//} \mathcal{X}$ 
14:      $\mathcal{L}_{\text{CPS}}^U \leftarrow \mathcal{L}_{\text{CPS}}^U + \mathcal{L}_{\text{CPS}}(\mathbf{P}_l^m, \mathbf{Y}_r) + \mathcal{L}_{\text{CPS}}(\mathbf{P}_r^m, \mathbf{Y}_l)$ 
15:   end for
16:   for  $i = 1, \dots, n$  do
17:      $\mathcal{L}_L \leftarrow \mathcal{L}_L + \mathcal{L}_L(\mathbf{P}_i^L, \mathbf{Y}^*)$ 
18:   end for
19:    $\mathcal{L} \leftarrow \mathcal{L}_L + \frac{\lambda}{(n-1)} \mathcal{L}_{\text{CPS}}^U$ 
20:    $\mathcal{L}.\text{backward}()$ 
21: end for

```

**Ensemble learning techniques.** In the language of ensemble learning, an *ensemble* is a set of weak learners (models trained independently), which together forms a strong model. During the  $n$ -CPS training process, there are  $n$  networks trained separately. In the original approach, the evaluation used only the results of the first network and discarded the other ones. While this approach alone was proven to generate state-of-the-art results, our empirical results show that including all the information from the trained networks is beneficial for performance. In the original CPS paper, the experiment showed that even in the last steps of learning, approximately 5% of pixels are labelled differently by the trained networks.

Therefore, we use the results of all the networks. It can be realised by taking the pixel-wise softmax of the output of each network and then combining the results in several ways. In this paper, we test two of them: max confidence (denoted as *mc*) and soft voting (*sv*). In the max confidence approach, we choose the result with the highest score. In other words, for each pixel, we choose the class from the most *confident* network. In the PyTorch-like notation, that max confidence voting is defined as:  $\text{softmax}(\mathbf{y}, \text{dim}=2).\text{max}(\text{dim}=0)$ , where the concatenated output of all networks  $\mathbf{y}$  is of shape  $(n, b, c, w, h)$  – representing consecutively number of the networks, batch size, number of classes, width and height. The soft voting approach is similar, but instead of choosing the class with the highest score, we sum the probabilities of all the networks. This is proportional to the weighted mean of the output of all networks. In the PyTorch-like notation that would translate to  $\text{softmax}(\mathbf{y}, \text{dim}=2).\text{sum}(\text{dim}=0)$ .

## 3 Evaluation

This section describes the evaluation of the proposed approach. First, we present the setup of our experiments and the training details. We evaluate  $n$ -CPS on PASCAL VOC 2012 and Cityscapes datasets. Ablation studies are also performed.

### 3.1 Experiment setup

**Datasets.** The datasets used in this experiment are the same as in the original CPS paper [Chen *et al.*, 2021] – PAS-

CAL VOC 2012 [Everingham *et al.*, 2010] and Cityscapes [Cordts *et al.*, 2016]. The PASCAL VOC 2012 contains 21 classes (including the background class). Regarding Cityscapes, it comprises 30 classes. We also follow GCT [Ke *et al.*, 2020] protocols regarding the ratio of supervised-to-unsupervised images in the dataset (1/16, 1/8, 1/4, 1/2). The sampling scheme is taken from the CPS paper [Chen *et al.*, 2021] to provide a fair comparison with other methods. Both datasets are evaluated using the standard mean intersection over union (mIoU) metric in % over val sets (1,456 images in PASCAL VOC 2012 and 500 in Cityscapes).

**Training details.** We use the same training setup as in the original CPS paper [Chen *et al.*, 2021]. We extend the original PyTorch codebase with our  $n$ -CPS approach, although training details (such as augmentations or hyperparameters) stays the same. This means that we use DeepLabv3+ [Chen *et al.*, 2018] as our network with ResNet-50/101 backbones [He *et al.*, 2016] paired with mini-batch SGD with momentum (0.9) and weight decay (0.0005). We also use the poly learning rate policy, in which the initial learning rate is multiplied by  $(1 - \frac{\text{iter}}{\text{max\_iter}})^{0.9}$ . For Pascal VOC, both supervised and CPS loss is computed using standard cross-entropy loss. Regarding Cityscapes, OHEM loss [Shrivastava *et al.*, 2016] is used for supervised loss and cross-entropy loss for CPS loss. VOC models were trained on  $4 \times V100$  GPUs, whereas Cityscapes models on  $8 \times V100$  GPUs.

## 3.2 Results

We report mIoU results from the network with the highest-scoring step (not necessarily the last one). These results use  $n = 3$  as the number of networks and `mc` and `sv` ensembling techniques<sup>2</sup>. The training regime is taken from the CPS paper, and it consists of different supervision ratios (1/16, 1/8, 1/4, 1/2) trained for 32/34/40/60 and 128/137/160/240 steps for Pascal VOC and Cityscapes, respectively. We report the best test results during the evaluation (not necessarily the result from the last step).

**Pascal VOC 2012.** The first part of Table 1 presents the results on the Pascal VOC dataset compared to other recent methods (the non-our results are taken from the CPS paper [Chen *et al.*, 2021]). For different supervision regimes (1/16, 1/8, 1/4, 1/2), the version without CutMix outperforms the mIoU results reported in the original CPS paper (previous state-of-the-art) by  $+0.15/+0.49/+1.57/+1.16$  percentage points for ResNet-50 and  $+1.33/+0.75/+1.06/+1.38$  pp for ResNet-101. Regarding the version with CutMix algorithm, the  $n$ -CPS approach is better than CPS by  $+0.05/+0.54/+0.95/+0.50$  pp for ResNet-50 and  $+1.38/+1.55/+1.29/+1.62$  pp for ResNet-101. Mean confidence and soft voting ensembles behave similarly, and usually, the difference is slight (not more significant than  $\pm 0.1$  mIoU). Interestingly, for ResNet-50, the ver-

<sup>2</sup>Our evaluation was primarily meant to be done on max confidence voting. Soft voting was added later and was tested only on the models that were best performing with the max confidence voting. This means that there is a chance that reported soft voting results might be slightly improved if tested on all steps.

sion without CutMix outperforms the version with CutMix. This effect is not observed with ResNet-101.

**Cityscapes.** The second part of Table 1 presents the results on the Cityscapes dataset compared with other recent methods. Simiraly, the non-our results are taken from the CPS paper [Chen *et al.*, 2021]. We do not report results for the ResNet-101 backbone network due to the unavailability of the appropriate hardware ( $8 \times V100$  GPUs were not enough in terms of RAM). On ResNet-50 and without CutMix,  $n$ -CPS achieved  $-0.01/+0.49/-0.11/+0.65$  pp change of mIoU compared to CPS. With CutMix on, our approach outperforms the current state of the art by  $+1.61/+1.00/+0.58/+0.43$  pp. Even without testing our apporach on ResNet-101, the  $n$ -CPS on ResNet-50 outperforms CPS on ResNet-101 on 1/16 supervision ( $+1.36$  mIoU). Interestingly, the model based on ResNet-50 with the CutMix algorithm showed a slightly worse performance 1/2 supervision than the model without it. This behaviour is consistent with the PASCAL VOC 2012 results.

## 3.3 Ablations

This section presents the ablation experiments on the Pascal VOC 2012 dataset. We try to assess the importance of generalising CPS by controlling the number of networks  $n$ . Then, we address the influence of the max confidence ensembling technique without cross-pseudo supervision. Finally, we study how the choice of ensembling technique influences the performance.

**Importance of  $n$ -CPS.** To assess the importance of  $n$ -CPS, we run a series of experiments on the PASCAL VOC 2012 dataset with different values. The results are reported in Table 2 in terms of the mIoU under different supervision regimes. We report the results of the original CPS [Chen *et al.*, 2021], as well as the results of our implementation ( $n$ -CPS, where  $n \in \{2, 3\}$ ). All networks were trained on DeepLabv3+ with ResNet-50/101 as a backbone and using  $\lambda = 1.5$ . Most importantly, we did not use any ensembling techniques here. Note that while the original CPS is equivalent to ours reproduced with 2-CPS, these results are slightly different due to randomness. Nevertheless, one can observe that evaluating only the first network  $f_1$  (as in the original CPS paper), which is not necessarily the best performing one, does not show the immediate advantage of using  $n$ -CPS (except ResNet-101 without CutMix).

**Importance of ensemble networks.** The previous paragraph showed that the choice of increased  $n$  does not improve the performance alone. However, in Section 3.2 we have already shown that the method combined with proper ensembling technique yields state-of-the-art results. To isolate the effect of ensembling, we performed a series of experiments with  $\lambda$  set to zero. This disabled cross-pseudo supervision loss from the learning process and effectively turned the task to standard supervised ensemble learning. Table 3 presents the results of this ablation study. As it turns out, for 2-CPS, ensembling resulted in  $+1.57$  pp to mIoU, while ensembling and CPS ( $\lambda = 1.5$ ) provided another  $+2.78$  pp for 1/16 supervised data. The trend is consistent in different supervision regimes, though it diminishes with larger shares of supervised

Table 1: Comparison of the semi-supervised segmentation methods (mIoU under different supervision regimes, DeepLabv3+).

	ResNet-50				ResNet-101			
	1/16	1/8	1/4	1/2	1/16	1/8	1/4	1/2
<i>Pascal VOC 2012</i>								
MT [Tervainen and Valpola, 2017]	66.77	70.78	73.22	75.41	70.59	73.20	76.62	77.61
CCT [Ouali <i>et al.</i> , 2020]	65.22	70.87	73.43	74.75	67.94	73.00	76.17	77.56
CutMix-Seg [French <i>et al.</i> , 2019]	68.90	70.70	72.46	74.49	72.56	72.69	74.25	75.89
GCT [Ke <i>et al.</i> , 2020]	64.05	70.47	73.45	75.20	69.77	73.30	75.25	77.14
CPS [Chen <i>et al.</i> , 2021]	68.21	73.20	74.24	75.91	72.18	75.83	77.55	78.64
CPS+CutMix [Chen <i>et al.</i> , 2021]	71.98	73.67	74.90	76.15	74.48	76.44	77.68	78.64
3-CPS-mc (ours)	68.36	73.45	75.75	77.00	73.51	76.46	78.59	79.90
3-CPS-sv (ours)	68.28	73.69	75.81	<b>77.07</b>	73.25	76.58	78.61	80.02
3-CPS-mc+CutMix (ours)	<b>72.03</b>	74.18	<b>75.85</b>	76.65	75.80	77.96	<b>78.97</b>	80.06
3-CPS-sv+CutMix (ours)	71.97	<b>74.21</b>	75.83	76.6	<b>75.86</b>	<b>77.99</b>	78.95	<b>80.26</b>
<i>Cityscapes</i>								
MT [Tervainen and Valpola, 2017]	66.14	72.03	74.47	77.43	68.08	73.71	76.53	78.59
CCT [Ouali <i>et al.</i> , 2020]	66.35	72.46	75.68	76.78	69.64	74.48	76.35	78.29
GCT [Ke <i>et al.</i> , 2020]	65.81	71.33	75.30	77.09	66.90	72.96	76.45	78.58
CPS [Chen <i>et al.</i> , 2021]	69.79	74.39	76.85	78.64	70.50	75.71	77.41	80.08
CPS+CutMix [Chen <i>et al.</i> , 2021]	74.47	76.61	77.83	78.77	74.72	77.62	79.21	80.21
3-CPS-mc (ours)	69.78	74.80	76.74	<b>79.29</b>	—	—	—	—
3-CPS-sv (ours)	69.76	74.88	76.74	79.27	—	—	—	—
3-CPS-mc+CutMix (ours)	76.06	77.58	78.36	79.15	—	—	—	—
3-CPS-sv+CutMix (ours)	<b>76.08</b>	<b>77.61</b>	<b>78.41</b>	79.2	—	—	—	—

data (+1.47/+2.04 pp for 1/8 supervised, +1.13/+1.44 pp for 1/4 supervised, +0.59/+0.42 pp for 1/2 supervised). Regarding 3-CPS, one can observe similar behaviour (+2.09 pp with ensembling and +2.08 pp with  $\lambda = 1.5$  for 1/16 supervised, +1.79/+1.88 pp for 1/8 supervised, +2.04/+0.72 pp for 1/4 supervised, +1.53/+0.02 pp for 1/2 supervised). This shows that the choice of ensembling and CPS positively affects the performance, especially compared to the ensembling alone. Regarding the  $n$  with ensembling, we observe that the performance of the 3-CPS-ens is better than 2-CPS (+0.11 pp for 1/8 supervised, +0.10 pp for 1/4 supervised, +0.27 pp for 1/2 supervised) except 1/16 supervised (−0.60 pp). This justifies the generalisation of the original CPS combined with ensembling for larger shares of supervised data.

**Importance of the ensemble learning method.** We also investigate how the choice of ensembling technique influences the performance during the whole training process. Apart from the best results reported in Table 1, we also control it in a full training procedure. To do so, we trained  $n$ -CPS ( $n = 3$ ,  $\lambda = 1.5$ ) with the 1/8 supervised regime with ResNet-50 on the Pascal VOC dataset and control evaluation results for different types of ensembling techniques presented in Section 2: no ensembling (i.e. only the first network is evaluated), max confidence and soft voting. Figure 3 shows the results of the ablation study. The highest mIoU scores were 73.85 for soft voting and 73.71 for max confidence. In this case, soft voting was better than max confidence by

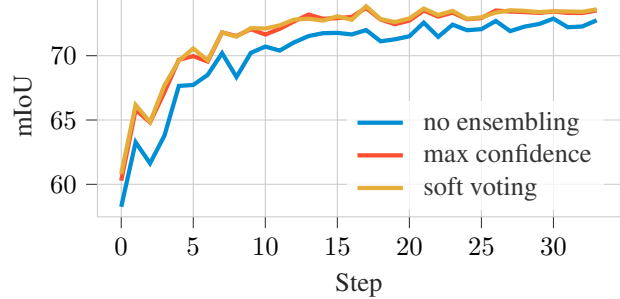


Figure 3: Ablation study of different ensembling methods for 3-CPS on Pascal VOC 1/8 supervised (ResNet-50, without CutMix).

0.11 mIoU points on average. Soft voting was also better on the majority of learning steps. Notice that these results are slightly different than the results reported in Table 1, as they were collected in a separate run.

## 4 Related Work

This section briefly describes other work in the areas of semantic segmentation and semi-supervised learning.

**Semantic segmentation.** Semantic segmentation is a fundamental problem in computer vision, which consider assigning labels to each pixel in an image. Modern deep neural networks successfully adapted to this problem, with

Table 2: Ablation study on the number of networks (no ensemble techniques, DeepLabv3+ with ResNet-50/101 backbone,  $\lambda = 1.5$ ).

	ResNet-50				ResNet-101			
	1/16	1/8	1/4	1/2	1/16	1/8	1/4	1/2
CPS (Chen <i>et al.</i> )	68.21	73.20	74.24	75.91	72.18	75.83	77.55	78.64
2-CPS (ours)	68.64	73.30	75.34	76.33	73.15	76.07	77.32	78.64
3-CPS (ours)	67.5	72.67	75.12	76.36	73.32	76.03	78.25	78.87
CPS+CutMix (Chen <i>et al.</i> )	71.98	73.67	74.90	76.15	74.48	76.44	77.68	78.64
2-CPS+CutMix (ours)	71.43	73.99	75.37	75.6	74.59	77.11	77.64	78.65
3-CPS+CutMix (ours)	71.11	73.56	74.68	75.86	74.98	76.98	77.95	79.67

Table 3: Ablation study on importance of CPS ( $\lambda \in \{0, 1.5\}$ ),  $n$ -CPS ( $n \in \{2, 3\}$ ) and ensembling (none, max confidence) on Pascal VOC (ResNet-50, without CutMix).

	$\lambda$	1/16	1/8	1/4	1/2
2-CPS	0	64.61	69.83	73.08	75.72
2-CPS-mc	0	66.18	71.3	74.21	76.13
2-CPS-mc	1.5	68.96	73.34	75.65	76.73
3-CPS	0	64.19	69.78	72.63	75.45
3-CPS-mc	0	66.28	71.57	75.03	76.98
3-CPS-mc	1.5	68.36	73.45	75.75	77.00

fully-convolutional networks (FCN) [Long *et al.*, 2015] being one of the first and most influential approaches. Many solutions follow the encoder-decoder architecture, such as U-Net [Ronneberger *et al.*, 2015]. Numerous techniques have been developed, such as pyramid scene parsing in PSPNet [Zhao *et al.*, 2017], or dilated convolutions and atrous spatial pyramid pooling as in DeepLabv3+ [Chen *et al.*, 2018]. Another architecture, HRnet [Wang *et al.*, 2020] is focused on keeping high-resolution representations during the training.

**Semi-supervised learning.** A recent line of research has shown that deep neural networks can be successfully used for semantic segmentation, given the right amount of data. From the practical point of view, this is a challenging problem due to the high cost of labelling. The goal of semi-supervised learning is to learn a model on a dataset, for which the labels are known on a certain percentage of the data. Semi-supervised learning combines semantic segmentation and semi-supervised learning. Recently, an intense effort can be observed in developing two families of techniques: contrastive learning and consistency regularisation. Contrastive learning is built around learning representations which are *close* for the samples of the same class and *far* otherwise. Consistency regularisation assumes that the same samples should yield the same labels under different – often heavy – augmentations and perturbations. The disagreement between models is later used for the training.

Apart from CPS [Chen *et al.*, 2021], there are several architectures dedicated to semi-supervised learning. A somewhat similar approaches are cross-consistency training (CCT) [Ouali *et al.*, 2020] or GCT [Ke *et al.*, 2020], which uses cross-confidence consistency for feature perturbation. Mean

Teacher [Tarpainen and Valpola, 2017] considers a setting in which two models (student and teacher) are trained on the same dataset but using different augmentations. The student model is trained in a standard way, while the teacher model is an exponential moving average of student models from previous steps. The latter is also responsible for generating pseudo labels. The Mean Teacher framework combined with CutMix [Yun *et al.*, 2019] was used for semi-supervised segmentation in CutMix-Seg [French *et al.*, 2019]. In Dynamic Mutual Training (abbreviated as DMT) [Feng *et al.*, 2020], two neural networks are trained using a dynamically re-weighted loss function. The authors of DMT leverages the disagreement between the models, which indicates a possible error and lowers the loss value. ReCo (an abbreviation from Regional Contrast) [Liu *et al.*, 2021] is a pixel-level contrastive learning framework, which incorporates memory-efficient sampling strategies. The framework proved to be very effective in few-supervision scenarios, reaching 50% mIoU on Cityscapes while requiring only 20 labelled images.

## 5 Summary

In this paper, we presented  $n$ -CPS – a generalisation of the consistency regularisation framework CPS. We also proposed to utilise all the learned subnetworks for evaluation purposes using the ensemble learning techniques. Evaluation of our approach on the Pascal VOC dataset showed that it sets the new state-of-the-art in its category. Future work should address the evaluation of the behaviour of models with  $n \geq 4$ . An unavoidable limitation of such a study stems from the large number of parameters involved in the models. In practical settings, this means relatively large GPU memory requirements. Moreover, further work should consider the evaluation of ResNet-101 on the Cityscapes dataset, as the results on ResNet-50 are promising.

## CRediT author statement

**Dominik Filipiak** (80% of the work): Conceptualisation, Methodology, Software, Validation, Formal Analysis, Investigation, Resources, Writing – Original Draft, Writing – Review & Editing, Visualization, Project Administration. **Piotr Tempczyk** (10% of the work): Conceptualisation, Funding Acquisition, Supervision, Writing – Review & Editing. **Marek Cygan** (10% of the work): Conceptualisation, Supervision, Resources, Writing – Review & Editing.

## References

[Chen *et al.*, 2018] Liang-Chieh Chen, Yukun Zhu, George Papandreou, Florian Schroff, and Hartwig Adam. Encoder-decoder with atrous separable convolution for semantic image segmentation. In *ECCV*, 2018.

[Chen *et al.*, 2021] Xiaokang Chen, Yuhui Yuan, Gang Zeng, and Jingdong Wang. Semi-supervised semantic segmentation with cross pseudo supervision. In *Proceedings of the IEEE/CVF Conference on Computer Vision and Pattern Recognition*, pages 2613–2622, 2021.

[Cordts *et al.*, 2016] Marius Cordts, Mohamed Omran, Sebastian Ramos, Timo Rehfeld, Markus Enzweiler, Rodrigo Benenson, Uwe Franke, Stefan Roth, and Bernt Schiele. The cityscapes dataset for semantic urban scene understanding. In *Proceedings of the IEEE conference on computer vision and pattern recognition*, pages 3213–3223, 2016.

[Everingham *et al.*, 2010] Mark Everingham, Luc Van Gool, Christopher KI Williams, John Winn, and Andrew Zisserman. The pascal visual object classes (voc) challenge. *International journal of computer vision*, 88(2):303–338, 2010.

[Feng *et al.*, 2020] Zhengyang Feng, Qianyu Zhou, Qiqi Gu, Xin Tan, Guangliang Cheng, Xuequan Lu, Jianping Shi, and Lizhuang Ma. Dmt: Dynamic mutual training for semi-supervised learning. *arXiv preprint arXiv:2004.08514*, 2020.

[French *et al.*, 2019] Geoff French, Timo Aila, Samuli Laine, Michal Mackiewicz, and Graham Finlayson. Semi-supervised semantic segmentation needs strong, high-dimensional perturbations. 2019.

[He *et al.*, 2016] Kaiming He, Xiangyu Zhang, Shaoqing Ren, and Jian Sun. Deep residual learning for image recognition. In *Proceedings of the IEEE conference on computer vision and pattern recognition*, pages 770–778, 2016.

[Ke *et al.*, 2020] Zhanghan Ke, Di Qiu, Kaican Li, Qiong Yan, and Rynson WH Lau. Guided collaborative training for pixel-wise semi-supervised learning. In *Computer Vision–ECCV 2020: 16th European Conference, Glasgow, UK, August 23–28, 2020, Proceedings, Part XIII 16*, pages 429–445. Springer, 2020.

[Liu *et al.*, 2021] Shikun Liu, Shuaifeng Zhi, Edward Johns, and Andrew J Davison. Bootstrapping semantic segmentation with regional contrast. *arXiv preprint arXiv:2104.04465*, 2021.

[Long *et al.*, 2015] Jonathan Long, Evan Shelhamer, and Trevor Darrell. Fully convolutional networks for semantic segmentation. In *Proceedings of the IEEE conference on computer vision and pattern recognition*, pages 3431–3440, 2015.

[Ouali *et al.*, 2020] Yassine Ouali, Céline Hudelot, and Myriam Tami. Semi-supervised semantic segmentation with cross-consistency training. In *Proceedings of the IEEE/CVF Conference on Computer Vision and Pattern Recognition*, pages 12674–12684, 2020.

[Ronneberger *et al.*, 2015] Olaf Ronneberger, Philipp Fischer, and Thomas Brox. U-net: Convolutional networks for biomedical image segmentation. In *International Conference on Medical image computing and computer-assisted intervention*, pages 234–241. Springer, 2015.

[Shrivastava *et al.*, 2016] Abhinav Shrivastava, Abhinav Gupta, and Ross Girshick. Training region-based object detectors with online hard example mining. In *Proceedings of the IEEE conference on computer vision and pattern recognition*, pages 761–769, 2016.

[Tarvainen and Valpola, 2017] Antti Tarvainen and Harri Valpola. Mean teachers are better role models: Weight-averaged consistency targets improve semi-supervised deep learning results. *arXiv preprint arXiv:1703.01780*, 2017.

[Wang *et al.*, 2020] Jingdong Wang, Ke Sun, Tianheng Cheng, Borui Jiang, Chaorui Deng, Yang Zhao, Dong Liu, Yadong Mu, Mingkui Tan, Xinggang Wang, et al. Deep high-resolution representation learning for visual recognition. *IEEE transactions on pattern analysis and machine intelligence*, 2020.

[Yun *et al.*, 2019] Sangdoo Yun, Dongyoon Han, Seong Joon Oh, Sanghyuk Chun, Junsuk Choe, and Youngjoon Yoo. Cutmix: Regularization strategy to train strong classifiers with localizable features. In *Proceedings of the IEEE/CVF International Conference on Computer Vision*, pages 6023–6032, 2019.

[Zhao *et al.*, 2017] Hengshuang Zhao, Jianping Shi, Xiaojuan Qi, Xiaogang Wang, and Jiaya Jia. Pyramid scene parsing network. In *Proceedings of the IEEE conference on computer vision and pattern recognition*, pages 2881–2890, 2017.